Pattern Recognition of Inter-Turn Short Circuit Fault in Wound Field Synchronous Generator via Stray Flux Monitoring

H. Ehya, *Student Member, IEEE*, A. Nysveen, *Senior, IEEE* , and R. Nilssen

***Abstract*—This paper provides a novel approach to discriminate the Inter-Turn Short Circuit fault (ITSC) in salient pole synchronous generator based on the use of non-invasive sensors. A stray magnetic field is used as a non-invasive signal that could provide valuable data regarding the condition of the synchronous machine. The captured signal under different severity of the ITSC fault is examined by using a classical signal processing tool based on Fast Fourier Transform. A unique feature based on extracted sub harmonics from the stray magnetic field is used to demonstrate the sensitivity of the signal to fault severity increment. It has been shown that the nominated feature do not have any sensitivity to the load variation. The theoretical hypothesis which is supported by using finite element method analysis is tested and verified by experimental results.**

***Index Terms*—Condition monitoring, fault detection, feature extraction, finite element modeling, pattern recognition, synchronous generator, stray magnetic field, spectrum analysis.**

I. Introduction

The inter-turn short circuit of the rotor field winding is critical and serious failure among various kind of faults in synchronous generators that can effect the operation of the machine. Although, the synchronous generators often operate well for decades in power plants, such faults can shorten their efficient life span. Therefore, it is proposed to use precise condition monitoring of the synchronous generators to reduce the possibility of the failure and generator outage.

The ITSC fault can occur due to electrical or mechanical problems in the field winding insulation. ITSC failure can give rise to local hot spot and vibrations that in turn can accelerate the insulation degradation [1]. Numerous approaches are proposed to detect the fault in synchronous machines which mostly relys on harmonic analysis of the stator terminal voltage [2], air gap magnetic field [3], phase currents [4], and vibrations in the frame [5]. Nevertheless, mentioned methods have some drawbacks like:

1) Although, the air gap magnetic field provides the valuable data to detect the ITSC, it is invasive approach and it is difficult to implement in synchronous generators that are already in operation.
2) Harmonics of the voltage, current, vibration show significant changes in the harmonic contents 'only' in a case of severe degree of ITSC fault.

In order to tackle the aforementioned problems, the stray magnetic field is proposed to detect the ITSC fault. It is a non-invasive approach and may demonstrate the high sensitivity to occurrence of the failure.

The magnetic field outside the machine is created by the leakage flux that can be captured by utilizing search coil, hall effect sensors, optical fiber [6], and radio frequency sensors [7]. The amplitude of the induced Electro Motive Force (EMF) in the search coil is proportional to the rate of leakage flux variation, and the number of turns. In addition, the distance between the search coil and the frame of the machine strongly influence the amplitude of the induced EMF. The location of the sensor could determine whether the measured signal is the axial flux, radial flux or both. The location of the sensor should therefor be chosen based on which stray flux must be investigated [8]. For instance, eccentricity faults in horizontally mounted synchronous generators can slightly change the value and the harmonic contents of the axial stray flux.

The present work has studied the application of the stray flux to diagnose the inter-turn short circuit fault in the field winding of the salient pole synchronous generator. The main target of this study is to see if this can provide a method with high precision and high degree of sensitivity to the lowest degree of ITSC fault. In section II, the comprehensive finite element analysis by using search coils are presented. It has shown that occurrence of the fault could change the variation of the induced EMF in the sensor. Spectrum analysis is used to characterise the induced sub harmonics in EMF under ITSC fault in section III. In section IV, the experimental set-up that is used to verify the accuracy of the theoretical findings is explained in detail. It is shown in section V that the load alternation does not has any effect on the nominated feature.

II. Finite Element Modeling and Analysis

The 2-D geometry of the simulated salient pole synchronous generator is displayed in Fig. 1. The detailed geometrical characteristics of the stator and rotor slots, nonlinearity of the stator lamination sheets, spatial distribution of the stator winding, and saliency of the rotor poles are

This work was supported by Norwegian Hydropower Centre (NVKS) and Norwegian Research Centre for Hydropower Technology (HydroCen).

Hossein Ehya, Arne Nysveen, and Robert Nilssen are with the Department of Electrical Power Engineering, Norwegian University of Science and Technology (NTNU), 7034 Trondheim, Norway. (e-mail: hossein.ehya@ntnu.no).

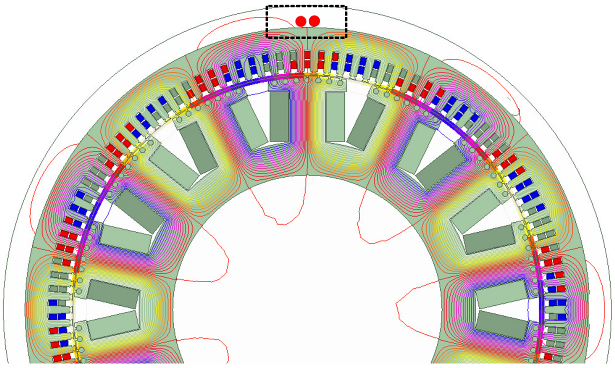

Fig. 1. Geometric configuration of the modelled salient pole synchronous generator using 2-D FEM. The location of the search coils are demonstrated in red circles.

TABLE I
100 kVA, Cosϕ 0.9, 400 V, 428 rpm, 14 Poles, Salient Pole Synchronous Generator

Quantity	***Values***
Stator outer diameter	780 mm
Stator inner diameter	650 mm
Number of stator slots	114
Length of stack	208 mm
Minimum air gap length	1.75 mm
Number of turns per coil	8
Number of turns per pole	35
Excitation current	88 A
Line current	148 A

considered since the accuracy of the fault features depends on the precision of the finite element model [9]. In addition, the winding arrangements in the stator and rotor have considerable impacts on fault detection since winding distribution affects the harmonic components of the magnetic field. In this modeling, a two-layer fractional slot stator winding and the corresponding spatial distribution are considered. A direct current according to the load level are fed into the rotor field windings.

The generator is modelled and analysed using ANSYS Maxwell [10]. A 2D-model is employed where the 3D-effects on stator and rotor windings are included using external circuits in the FEM-model. The simulation are made in the time domain until a steady-state is reached in the simulation. Rotation is included in the simulation. The non-linearity of the steel in both rotor and stator is included, but the eddy-current effects are disregarded except in the damper bars.

In order to capture the radial stray flux of the machine a flux sensor which is a stranded search coil is mounted on stator core. The amplitude of the magnetic field on the stator core is insignificant to the total number of turns for the designed flux sensor. The flux sensor has considered to be 3000 turns in order to capture the induced EMF from the stray magnetic field. Short-circuited turns in the field winding were simulated by simply reducing the total number of conductors in the field winding of a desired pole while applying the specified excitation currents at no-load or load conditions to the field winding. The specification of the proposed three-phase synchronous generator have been summarized in Table I.

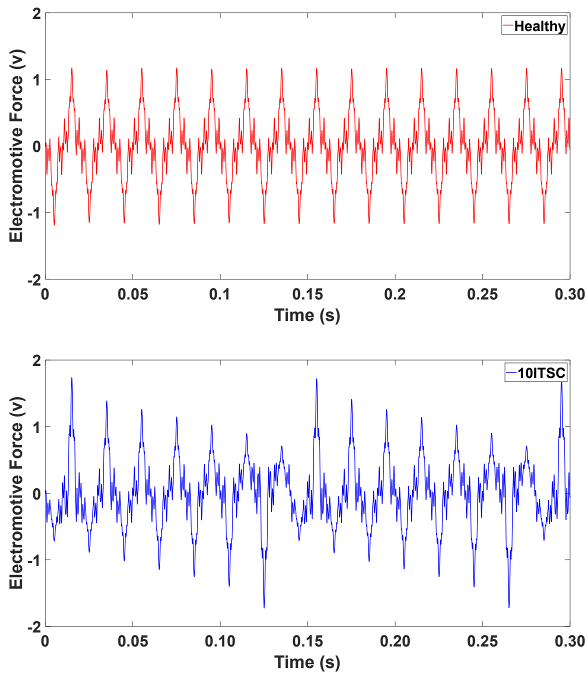

Fig. 2. Induced electromotive force in the sensor due to stray flux variation in the healthy (top) and 10 ITSC fault (bottom) - Simulation result.

TABLE II
The Number and Percentage of Shorted Turns in the Faulty Pole of the Salient Pole Synchronous Generator

Number of Turns	***Total Percentage per Pole***	***Total Percentage per Total Poles***
0 turn	Healthy	Healthy
1 turn	2.86%	0.204%
2 turns	5.71%	0.408%
3 turns	8.57%	0.612%
7 turns	20%	1.428%
10 turns	28.57%	2.045%

Fig. 2 shows the magnitude of the induced EMF due to stray flux density variation in the back iron of the synchronous generator for the healthy and 10 ITSC fault in no-load condition. As shown in Fig. 2, the inter-turn short circuit fault leads to variation in the amplitude of induced EMF. When a short circuit fault occurs, the effective number of field windings decreased which results in the reduction of net magneto-motive force in the air gap. Such an unbalanced distribution of the magneto-motive force leads into the asymmetric air gap magnetic field.

The unbalanced magnetic field is due to fundamental MMF components from the stator and rotor. In addition, the stator and rotor permeances variations together with the short circuit harmonic components strongly influence the resulting flux density distribution. The harmonic components created in the air gap magnetic field are also accessible in the stray flux because the fault could distort the inductance of the synchronous machines and it leads into considerable changes in the leakage flux that pass through the yoke to the air and

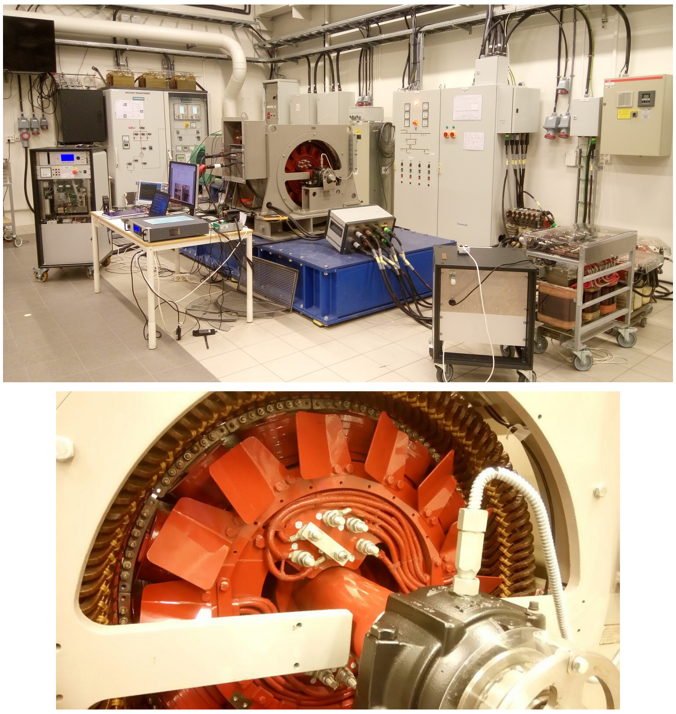

Fig. 3. The experimental set-up of 100 kVA custom-made synchronous generator for the purpose of fault detection (top), the rotor of the generator and the taps of field winding to apply ITSC fault.

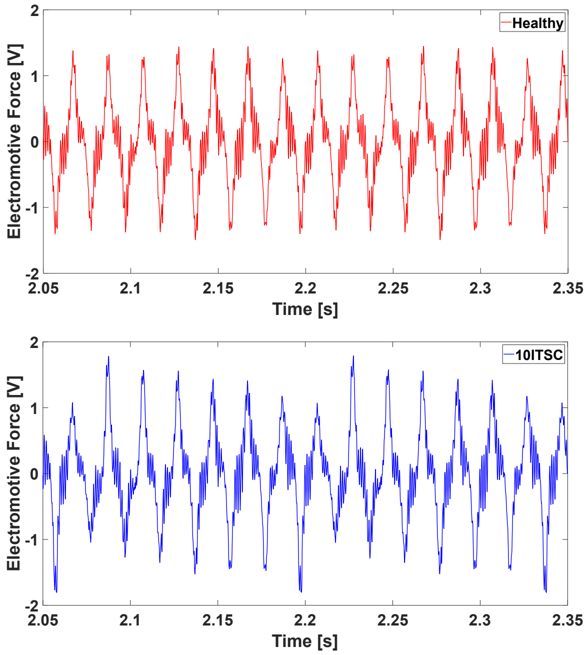

Fig. 4. Induced electromotive force in the sensor due to stray flux variation in the healthy (top) and 10 ITSC fault (bottom) - Experimental result.

the flux sensor. By increasing the severity of inter-turn short circuit fault, the amplitude and variation of the stray flux is increased.

III. Experimental Set-up

To investigate the synchronous machine performance under inter-turn short circuit fault, the following experimental components were provided:

1) A custom made 100 kVA, 14 poles, 400 V salient pole synchronous generator with detailed specification given in Table I.
2) A 90 kW induction motor with four poles and rated speed of the 1482 rpm were used as a prime mover of the synchronous machine.
3) The prime over is connected to the synchronous machine by using a gearbox.
4) The rotor field winding was supplied by a 200 kW LAB-HP/E2020 DC power source. The output of the DC power supply is 200 V and 1000 A.
5) A programmable converter is used to feed the induction motor based on its parameters. A rectifier connected to the grid was used to supply the converter.
6) Digitizing and sampling of the sensor measurement was performed by a high resolution 16-bit oscilloscope.
7) The water-cooled resistors comprised of two parallel sets of resistors, whereas the total resistance could be controlled and adjusted in steps by contactors and relays from the control panel. The per-phase resistance could be varied from a maximum of 160 Ω to a minimum of about 2.78 Ω. At the maximum load setting, the dissipated power of the resistors amounted to about 57 kW.
8) Two three-phase indicators that each of their phases were linked in series was connected to the synchronous generator by a three phase transformer. The transformer has a star to delta connection. The approximate value of the inductance in each phase based on the turn ratio of the transformer is equal to 22 mH.
9) A rigid flux sensor was used to capture the induced electromotive force due to stray flux. The sensor was installed on stator core to capture the stray radial flux of the machine. Although, the laboratory working environment is vulnerable to noise from converters, the frequency band of interest for flux sensor does not coincide with noise frequency range emitted from converters. Therefore, filter for noise rejection was not implemented in procedure of sensor design.

An experimental test rig of a synchronous generator is shown in Fig. 3. This system can be used to measure the air gap magnetic field by hall effect sensors that are installed on the stator tooth. The generator windings are star-connected, and the neutral point is grounded. The passive loads are used for generator loading condition in order to avoid grid harmonics interference on measured data. The main parts of the experimental test rig are as below:

The short circuit fault is applied to one of rotor poles , although there is a possibility to apply the inter turn short circuit fault to two opposite poles of a rotor field winding for different severity levels as shown in Table II. A copper plate is used in order to remove the desired number of turns

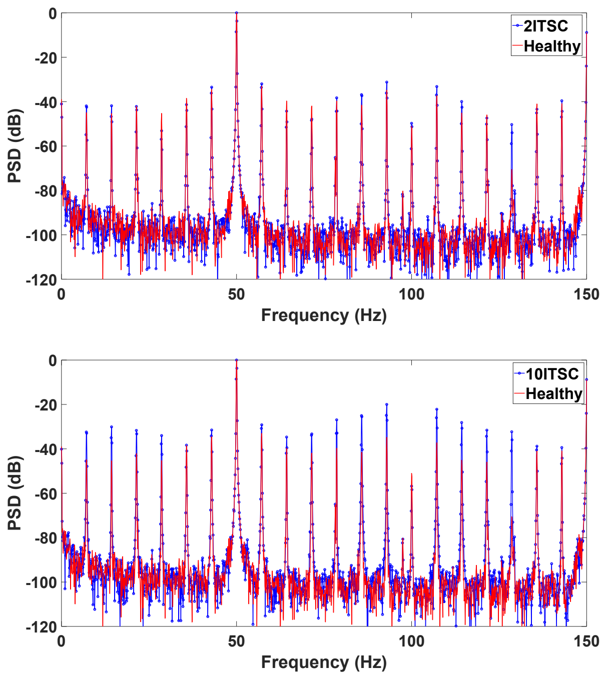

Fig. 5. The spectrum density of the induced EMF in the sensor in no-load for healthy and 2 ITSC fault (top), and healthy and 10 ITSC fault (bottom) - Experimental results.

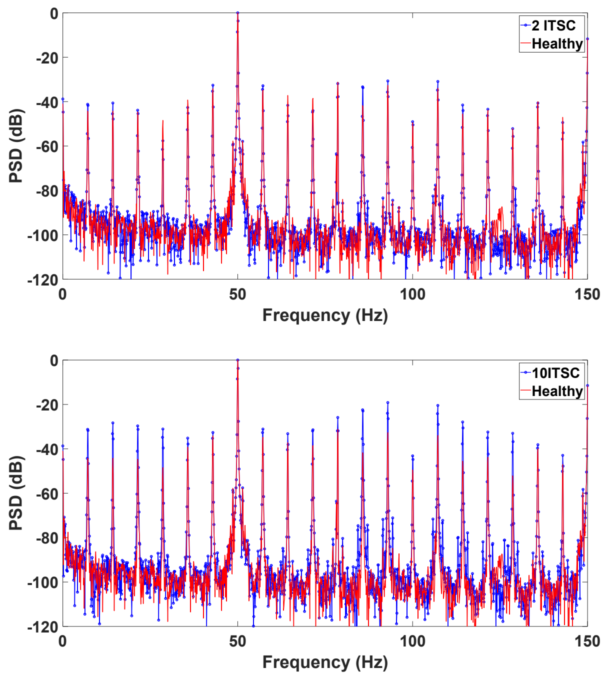

Fig. 6. The spectrum density of the induced EMF in the sensor in full-load for healthy and 2 ITSC fault (top), and healthy and 10 ITSC fault (bottom) - Experimental results.

in faulty pole. In a healthy case, the number of turns in one pole is 35 and the desired number of short circuit turn is achieved by using a copper plate between a common point of a field winding and desired turns point as shown in Fig. 3.

IV. Spectrum Analysis of Stray Flux

Fig. 5 depicts the power spectrum density (PSD) of the healthy and faulty synchronous generator with 2 (top) and 10 (bottom) ITSC. A comparison between the healthy and 2 ITSC faults illustrate that the presence of the fault increases the side-band components amplitude around the main frequency according to Equation. 1 as below:

$$f_{sideband} = (\frac{p \pm k}{p}) f_s \tag{1}$$

where p is number of pole pairs, f_s is a main frequency, and k is any integer. These side-bands components are equal to mechanical frequency that for a 14 pole synchronous generator with frequency of 50 Hz are equal to 7.1, 14.2, 21.3 Hz, and so forth. As seen in Fig. 5 the amplitude of all side-bands do not increase significantly for frequencies specially for low degree of fault severity. However, there is a regular pattern in which all frequency components around the fundamental frequency and its multiplier like 50, 100, 150 Hz are having a significant increase when a fault occur - even in its early stage. The mentioned frequencies are like 85.7, 92.9, 107.2, and 114.3 Hz. According to Fig. 5, the amplitude of aforementioned frequencies are -41.5, 34.8, -37.2, and -45.1 dB respectively. The occurrence of 1 ITSC fault in one of rotor field winding which is equal to 2.86% out of one rotor pole winding and 0.2% out of whole rotor field winding increase the magnitudes of mentioned frequencies to -39.4, -33.1, -35.1, and -42.8 dB. According to Fig. 5, the side-bands amplitude with 10 ITSC at frequency 85.7, 92.9, 107.2, 114.3 Hz increases from -41.7, -32.6, -33.9, and -45.5 dB to -22.4, -19.2, -20.4, and -27.9 dB, respectively. Therefore, the comparison between the healthy and faulty cases shows a considerable changes in the amplitude of the proposed index even with 1 ITSC. The variation of the extracted feature to severity of the ITSC fault in no-load condition are shown in Table II.

Fig. 6 demonstrates the frequency spectrum of the stray flux of the healthy and faulty synchronous generator at full load. Similar to the no-load condition, the harmonic components of the frequency spectrum in full load indicates the same degree of sensitivity to the occurrence and progress of the fault. For instance the proposed side-bands for 1 ITSC at frequency 85.7, 92.9, 107.2, and 114.3 Hz increase from -41.7, -32.6, -33.9, and -45.5 dB to -36.8, -32.1, -32.6, and -43.7 dB, respectively. There is also a significant increment in amplitude of the mentioned frequencies to -22.4, -19.2, -20.4, and -27.9 dB by increasing the severity of the fault to 10 ITSC. It shows that the load can not fluctuate or mask the proposed side-bands. Comparison between Figs. 5 and 7 shows that the amplitude of the side-band components, obtained by utilizing the finite element method is close to experimental results, which validate the simulated results and theoretical study.

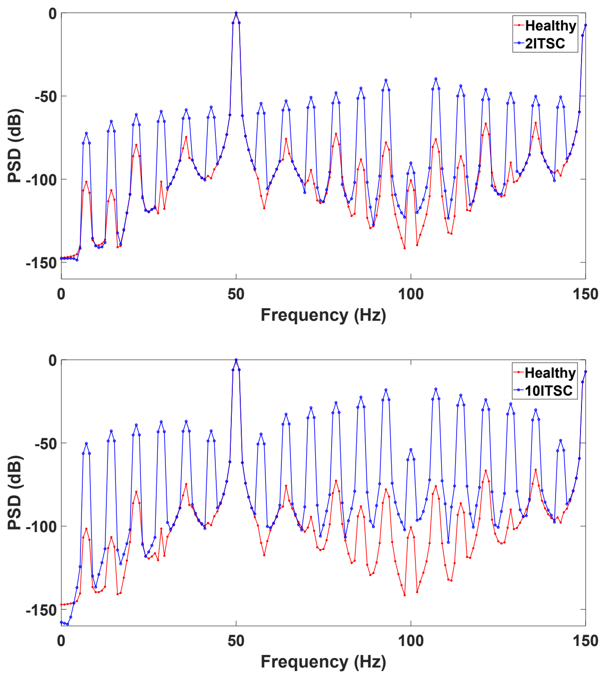

Fig. 7. The spectrum density of the induced EMF in the sensor in no-load for healthy and 2 ITSC fault (top), and healthy and 10 ITSC fault (bottom) - Simulation results.

V. Load Effects on the Proposed Feature

The investigation of the load variation on any proposed fault indices are essential. An accurate fault detection depends on the relationship between the suggested feature, load variation, and fault severity. It has been shown in [11] that the amplitude of the harmonic side-bands in induction motors, in the presence of eccentricity fault, under load condition is increased. Besides, the amplitude of the harmonic components of the faulty induction motor with broken damper bars fault is decreased by increasing the load level [12]. Consequently, the comparisons of healthy and faulty machine must be scrutinized in the same loads.

Fig.8 depicts the variation of proposed feature for different level of ITSC severity versus the load variation. According to Fig. 8, the amplitude of the mentioned criteria increases when increasing the number of shorted turns in the rotor field winding and it is reasonably constant from no-load to full-load. In other words, when using the proposed method based on utilizing the stray flux this is robust against the load variation. Therefore, short circuit fault detection based on nominated feature does not need to specify the generator's load.

VI. Conclusion

The stray magnetic field is used to detect the ITSC fault in the rotor field winding of the salient pole synchronous generator. Finite element modeling is used to simulate a 100 kVA SPSG under a short circuit fault. It has been shown that location, distance and the number of turns are the main

TABLE III
The Variation of Extracted Side-bands Components in Hz to Number of ITSC in No-Load in Decibel

Index	*H*	*1 ITSC*	*2 ITSC*	*3 ITSC*	*7 ITSC*	*10 ITSC*
7.1	-44.9	-43.6	-41.9	-40.3	-34.8	-32.4
14.3	-45.4	-43.9	-41.8	-39.7	-33.1	-30.1
85.7	-41.5	-39.4	-36.8	-34.5	-27.9	-25.0
92.9	-34.8	-33.1	-31.2	-29.9	-22.9	-19.9
107.2	-37.2	-35.1	-33.2	-31.4	-25.0	-22.1
114.3	-45.1	-42.8	-39.9	-37.5	-31.0	-28.1

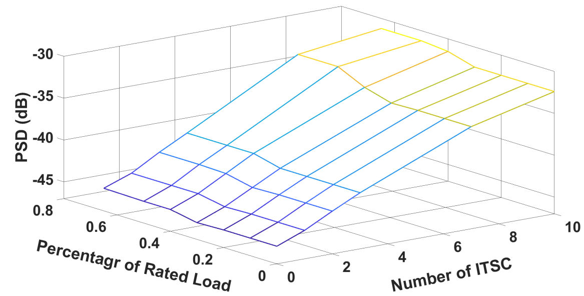

Fig. 8. Amplitude variation of side-band component versus load variation and various number of ITSC fault.

criteria for capturing the induced EMF in the installed search coil on the body of the machine. The severity of the fault and its impacts on the stray magnetic field has been studied and it is shown that it has high degree of sensitivity to the severity of the fault and it could even detect the 1 turn short circuit fault. The traditional signal processing tool is used in order to reduce the computational time and have a real time analyzer to extract the harmonic component of the signal. It has also been shown that side-band harmonics near the main frequency and its multipliers increase significantly by the occurrence and increment of the ITSC fault. The load effect on the extracted feature is also studied and it is proved that the load variation does no have any effect on the signature. The results have been verified by experimental results.

VII. Acknowledgment

The authors gratefully acknowledge the contributions of Dominik Håger, and Aksel Hanssen for their work on the preparation of the experimental test-rig.

References

[1] I. Sadeghi, H. Ehya, J. Faiz, and A. A. S. Akmal, "Online condition monitoring of large synchronous generator under short circuit fault—a review," in *2018 IEEE International Conference on Industrial Technology (ICIT)*. IEEE, 2018, pp. 1843–1848.

[2] S. E. Dallas, A. N. Safacas, and J. C. Kappatou, "Interturn stator faults analysis of a 200-mva hydrogenerator during transient operation using fem," *IEEE Transactions on Energy Conversion*, vol. 26, no. 4, pp. 1151–1160, Dec 2011.

[3] G. C. Stone, M. Sasic, J. Stein, and C. Stinson, "Using magnetic flux monitoring to detect synchronous machine rotor winding shorts," in *2011 Record of Conference Papers Industry Applications Society 58th Annual IEEE Petroleum and Chemical Industry Conference (PCIC)*, Sep. 2011, pp. 1–7.

[4] P. Neti, A. B. Dehkordi, and A. M. Gole, "A new robust method to detect rotor faults in salient-pole synchronous machines using structural asymmetries," in *2008 IEEE Industry Applications Society Annual Meeting*, Oct 2008, pp. 1–8.
[5] M. Cuevas, R. Romary, J. Lecointe, and T. Jacq, "Non-invasive detection of rotor short-circuit fault in synchronous machines by analysis of stray magnetic field and frame vibrations," *IEEE Transactions on Magnetics*, vol. 52, no. 7, pp. 1–4, July 2016.
[6] J. M. Corres, J. Bravo, F. J. Arregui, and I. R. Matias, "Unbalance and harmonics detection in induction motors using an optical fiber sensor," *IEEE Sensors Journal*, vol. 6, no. 3, pp. 605–612, June 2006.
[7] J. G. Mueller and T. G. Pratt, "A radio frequency polarimetric sensor for rotating machine analysis," *IEEE Sensors Journal*, vol. 13, no. 12, pp. 4866–4873, Dec 2013.
[8] A. Ceban, R. Pusca, and R. Romary, "Study of rotor faults in induction motors using external magnetic field analysis," *IEEE Transactions on Industrial Electronics*, vol. 59, no. 5, pp. 2082–2093, May 2012.
[9] B. M. Ebrahimi, M. J. Roshtkhari, J. Faiz, and S. V. Khatami, "Advanced eccentricity fault recognition in permanent magnet synchronous motors using stator current signature analysis," *IEEE Transactions on Industrial Electronics*, vol. 61, no. 4, pp. 2041–2052, 2013.
[10] A. Maxwell®, Release 2019 R3.7, ANSYS, Inc.
[11] J. Faiz, B. M. Ebrahimi, B. Akin, and H. A. Toliyat, "Comprehensive eccentricity fault diagnosis in induction motors using finite element method," *IEEE Transactions on Magnetics*, vol. 45, no. 3, pp. 1764–1767, 2009.
[12] A. M. Da Silva, R. J. Povinelli, and N. A. Demerdash, "Induction machine broken bar and stator short-circuit fault diagnostics based on three-phase stator current envelopes," *IEEE Transactions on Industrial Electronics*, vol. 55, no. 3, pp. 1310–1318, 2008.

VIII. BIOGRAPHIES

Hossein Ehya (S'19) received the M.Sc. degree in electrical engineering from the Department of Electrical and Computer Engineering, University of Tehran, Tehran, Iran, in 2013. From 2013 to 2018, Ehya worked as a electrical design engineer in electrical machines companies. He is currently working toward the Ph.D. degree in electrical engineering with Norwegian University of Science and Technology (NTNU), Trondheim, Norway. He is working on electromagnetic analysis and fault detection of synchronous machines. His research intrests include signal processing, pattern recognition, design, modeling, and fault diagnosis of electrical machines.

Arne Nysveen (M'98–SM'06) received his Dr.ing. in 1994 from Norwegian Institute of Technology (NTH). From 1995 to 2002 Nysveen worked as a research scientist at ABB Corporate Research in Oslo, Norway. Since 2002 Nysveen has been a professor at the Norwegian University of Science and Technology (NTNU). He is in charge for the turbine and generator technology research in the Norwegian Research Centre for Hydropower Technology (HydroCen).

Robert Nilssen received his Dr.ing. degree in 1989 from the Norwegian Institute of Technology (NTH). From 1989 to 1996 Nilssen worked at NTH as associated professor. In this period he was scientific advisor for SINTEF. Since 1996 Nilssen has been a professor at the Norwegian University of Science and Technology (NTNU) - with numerical electromagnetic field calculations as his main responsibility. In this period Nilssen has participated in a series of research projects in which design and optimization has been important. Nilssen has also been co-founder of several industry companies. He has been scientific advisor for several companies and in particular for SmartMotor AS and Rolls-Royce Norway - focusing on marine and aviation applications of Permanent Magnet Machines.